Journal of Thermal Analysis, Vol. 47 (1996) 1419-1436

INFLUENCE OF HEATING AND COOLING RATES ON THE GLASS TRANSITION TEMPERATURE AND THE FRAGILITY PARAMETER OF SORBITOL AND FRUCTOSE AS MEASURED BY DSC

D. Simatos, G. Blond, G. Roudaut, D. Champion, J. Perez[1] *and A. L. Faivre*[1]

ENSBANA - Campus Universitaire - 1, Esplanade Erasme - 21000 Dijon
[1]Laboratoire GEMPPM, CNRS-INSA - bat.502 - 69621 Villeurbanne, France

Abstract

The glass transition temperatures of sorbitol and fructose were characterized by four points determined on DSC heating thermograms (onset, mid-point, peak and end-point), plus the limit fictive temperature. The variations of these temperature values, observed as functions of cooling and heating rates, were used to determine the fragility parameter, as defined by Angell [1] to characterize the temperature dependence of the dynamic behavior of glass-forming liquids in the temperature range above the glass transition.

The apparent activation energy values, determined for the different temperatures studied, were similar for fructose and sorbitol. These values were compared to data obtained from other techniques, such as mechanical spectroscopy. The variations of the apparent activation values, observed in experiments involving cooling and heating at the same rate, slow cooling followed by rate-heating, or rate-cooling followed by fast heating, were explained by aging effects occurring during the heating step.

Keywords: cooling/heating rate, DSC, fragility parameter, glass transition temperature, sorbitol-fructose

Introduction

During the last several years, the temperature of the glass transition (T_g) has become a popular parameter in food science and technology. The curve representing the variation of the glass transition temperature with water content is the basis for the construction of state diagrams or stability maps of food components or food products [2–7]. This T_g curve is argued [2–6] to separate a zone of temperature and water content where a system can be expected to be kinetically stable from another zone where physical, chemical or biological changes, whose rates are diffusion-controlled, should occur with rates varying with temperature, according to WLF [8] kinetics.

0368–4466/96/ $ 5.00

John Wiley & Sons, Limited
Chichester

For a reliable application of these principles, however, two problems, at least, should be considered. A first problem is that, because of the dynamic character of the glass transition process, the value of T_g depends on the time characteristics of the measurement, and of the thermal history of the studied material [9–12]. Secondly, it is increasingly realized that the so-called "universal coefficients" (C_{1g}, C_{2g}) in the WLF equation [8] are only average values of the fitting parameters that were determined for some polymers. For a reliable prediction of the kinetics at temperatures above T_g, parameters specific to the behavior of the studied material should be used. A solution to this problem appears to be the fragility parameter, proposed by Angell [1, 13, 14] to characterize the temperature dependence of molecular mobility above T_g, and which can be determined from differential scanning calorimetry (DSC) mea-surements performed at various cooling/heating rates.

The purpose of this paper is to discuss the influence, on the T_g value and on the fragility parameter, of the cooling/heating rates used in DSC. The materials that have been chosen as examples are sorbitol and fructose, two substances having slightly different molecular structures, but T_g values in the same temperature range.

Background

The observable changes in physical properties, which are associated with the glass transition, are macroscopic processes accompanying a structural relaxation, i.e. a "kinetically impeded rearrangement of the structure of a liquid in response to changes in temperature" (or other imposed perturbations) [11]. The time scale for structural relaxation (τ) increases rapidly with decreasing temperature. The glass transition region is the temperature range where this relaxation time is similar to the experimental time scale (a few seconds or a few minutes, for usual laboratory measurements) [11].

T_g is most commonly determined *via* differential thermal analysis (DTA) or DSC during heating. Figure 1 shows typical DSC curves, obtained for sorbitol using two different heating rates. The glass transition appears as a change in heat capacity $(\Delta C_p)_{T_g}$, most often associated with an overshoot peak. These heat-capacity curves are the derivative curves of the enthalpy/temperature curves also shown on Fig. 1, and which were calculated by integration of the DSC traces. The first problem to be solved is to decide which of the temperatures that can be measured on the DSC curves (Fig. 1) should be determined as T_g. The mid-point of the heat-capacity jump (T_m) is very commonly considered as T_g, because it appears to be less sensitive to uncertainties in the baseline. Actually, this point is accepted as the standard T_g, as determined by DSC [15], although it does not have a clear physical meaning. Two other points could be preferred from the point of view of physical meaning: i) the onset point (T_o),

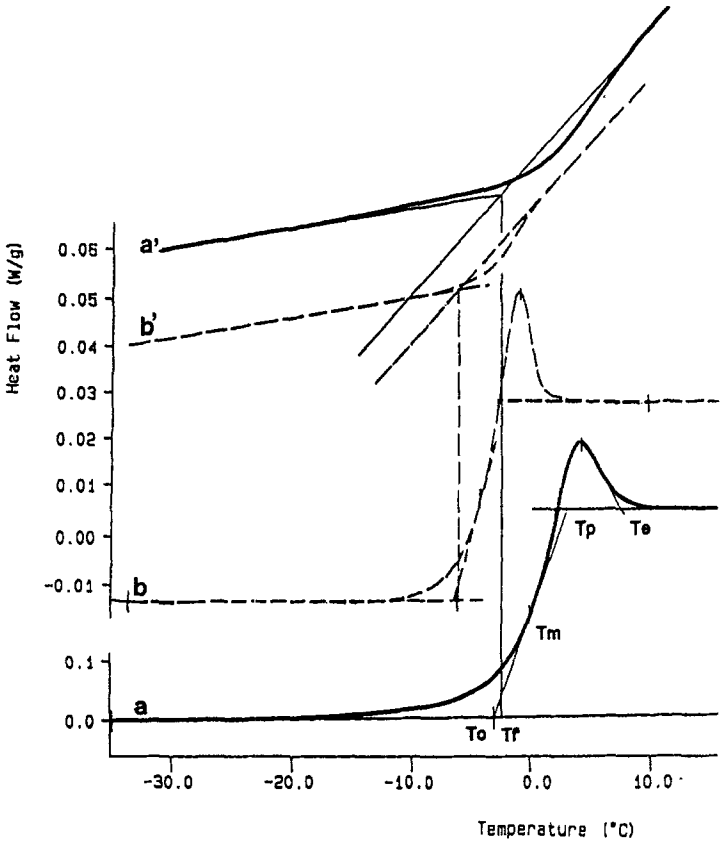

Fig. 1 DSC heating curves for sorbitol, after cooling carried out at the same rate: a) $q_c=q_h=20$ K min^{-1}; b) $q_c=q_h=2.5$ K min^{-1}. This figure illustrates the determination of the temperatures T_o, T_m, T_p, T_e. Curves a' and b' are the integrated curves of the thermograms, used for the determination of the temperature, T_f'

being the temperature at which the change from the glassy state towards the supercooled melt is becoming detectable; or ii) the end-point (T_e), being the temperature at which a metastable equilibrium can be considered to be reached [12].

Moreover, not only is T_g changing with the heating rate, but the shape of the DSC curve (and also the characteristic temperature values) depends on the whole thermal history of the sample (cooling rate; temperature and time of annealing below T_g) [9–12]. To obtain a T_g closest to the definition given previously, the best approach would be to determine it during a cooling experiment. Reports of T_g values determined *via* DSC or DTA during cooling are extremely scarce. This appears to be due to difficulties in obtaining reliable thermograms under these conditions, probably because temperature variation is not as accurately controlled during cooling as during heating. Moreover, the

temperature-scale calibration during cooling still appears to be problematic, although it has been claimed that this could be successfully carried out using liquid crystals as standards [16]. For these reasons, the glass transition is most often observed on heating in DSC experiments.

The limit fictive temperature is considered [9, 17] as a solution to this problem. The fictive temperature, T_f, of a material existing at an actual temperature, T, can be defined as the temperature at which the material in the equilibrium state would have the same enthalpy (H_e) as that corresponding to its structural or configurational state (Fig. 2). The limit fictive temperature, T_f', is the fictive temperature corresponding to the glass transition [9, 11, 18]. The interesting thing about this parameter is that it can be viewed as representing the structural/configurational state of the glass, as determined by its whole previous thermal history (cooling rate and annealing). If measured after a simple cooling, it appears to be equivalent to the T_g measured on cooling.

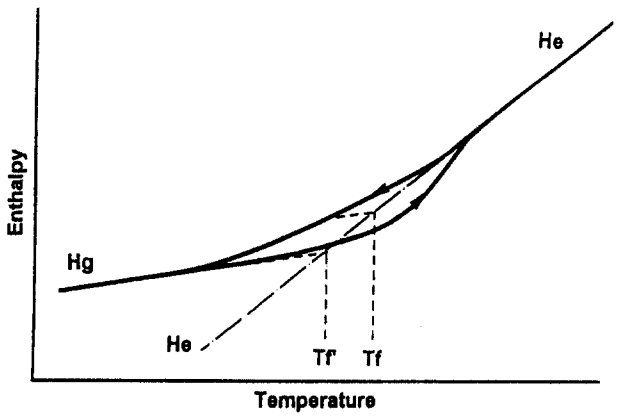

Fig. 2 Schematic change in enthalpy during cooling and immediate reheating at the same rate through the glass transition region. T_f=fictive temperature, T_f'=limit fictive temperature, H_e=change in enthalpy for the supercooled liquid in metastable equilibrium, H_g=change in enthalpy for the glass

The fragility parameter (m) was proposed by Angell [1, 13, 14] as a basis for the classification of supercooled materials according to the variation of their dynamic properties in the temperature range above T_g. By definition, m is the slope at T_g of the viscosity (or other dynamic property) in an Arrhenius plot, where the abscissa is scaled to the T_g of the material. Strong materials are those for which the temperature coefficient for the property under study (i.e. the slope of the curve) does not vary very much when the temperature is raised above T_g; they show behavior closest to Arrhenius behavior. Fragile materials, on the contrary, exhibit a rapid degradation of their mechanical properties, and then of their microstructure [1, 13, 14].

The relationships between m and the coefficients of the VFT and WLF equations can be written as follows. For the VFT equation [19–21]:

$$\eta = \eta_o \exp \frac{B}{T - T_o} \tag{1}$$

$$m = 16 + \frac{590T_o}{B} \quad \text{or} \quad m = 17 + \frac{666T_o}{B} \tag{2}$$

when the studied property is the relaxation time or the viscosity, respectively [14]. For the WLF equation [8]:

$$\log \frac{\eta}{\eta_{T_g}} = \frac{C_{1g}(T - T_g)}{C_{2g} + T - T_g} \tag{3}$$

$$m = \frac{C_{1g}T_g}{C_{2g}} \tag{4}$$

B, T_o, C_{1g}, C_{2g} and η_o are phenomenological coefficients; η and η_{T_g} are viscosities at T and T_g, respectively. It is possible to calculate m from the above expressions. Most often, however, viscosity measurements are limited to a range of low viscosities (10^2–10^7 Pa.s), i.e. to a temperature range remote from T_g. Although the validity of the VTF law has been demonstrated to extend down to the vicinity of T_g for a number of materials [22], by means of a combination of various techniques, the extrapolation may always be open to question.

Moreover, Eq.(2) is based on the assumption [14] that $\log\eta_{T_g}/\eta_o) = ct \approx 17$ (which also means that $C_{1g} \approx 17$).

DSC measurements of T_g, carried out at different cooling/heating rates, allow the determination of m. According to [16, 23]:

$$\ln q = -\frac{\Delta h}{RT_g} \tag{5}$$

where q is the cooling/heating rate in a DSC experiment, and Δh is the apparent activation energy for enthalpy relaxation.

Then, based on the definition of m, the value of m is obtained from [24]:

$$m = -\frac{\Delta h}{2.303RT_g} \tag{6}$$

Materials and methods

Sorbitol and fructose (analytical reagent grade) were obtained from Merck and used as supplied. About 10 mg of crystalline material were weighed in DSC volatile-sample pans, which were immediately sealed. After heating at 10 K min^{-1} to a temperature just above the melting point of the material, the sample was

cooled at the same rate of 10 K min^{-1} to just above the T_g range. The supercooled material was then subjected to various cooling/heating cycles. The heating scan immediately followed the cooling step.

DSC experiments were carried out with Perkin-Elmer DSC-7 equipment. Two-point temperature calibration was carried out for each heating rate employed in the experiment, using the crystal transition temperature of cyclohexane (186 K) and the melting temperature of indium (429.7 K). These calibrations were checked against the melting temperature of distilled water. Energy calibration was performed using the heat of melting of indium (28.45 J g^{-1}).

Three types of cooling/heating cycles were carried out. In the experiment "$q_c=q_h$", the same rates (1.25, 2.5, 5, 10 and 20 K min^{-1}) were used for both the cooling and the rewarming steps. In the experiment "q_h", a slow cooling (1.25 K min^{-1}) was followed with rate-heatings (1.25 to 20 K min^{-1}). In the experiment "q_c", after a cooling step performed at varying rates (1.25 to 20 K min^{-1}), a uniform heating rate (10 K min^{-1}) was applied.

The various temperature values (T_o, T_m, T_p and T_f') were determined using the Perkin-Elmer software. T_e was determined manually from the DSC curves. The slopes of the Arrhenius plots representing $\log q_h$ (or q_c) as a function of $1/T$ were calculated using the least-square linear-regression procedure of Excel 5 (Microsoft).

Mechanical spectroscopy measurements were carried out using a Metravib Viscoanalyser. Melted sorbitol was poured into the annular-shear device. After cooling at 2 K min^{-1} to a temperature at least 30 K below the T_g range, measurements were performed stepwise every 2 K during rewarming. The heating rate between the steps was 1 K min^{-1}; a stabilization time of 5 min was used before the measurements. Storage (G') and loss (G'') moduli were measured over a range of frequencies: 5–100 Hz.

Results

The variations of the various temperatures as functions of the tested cooling/heating rates are shown in Figs 3, 4 and 5 as "Arrhenius" plots. The slopes of the linear-regression lines are reported in Table 1 as apparent activation energies (Δh). The temperature values measured for a heating rate, q_h= 1.25 K min^{-1}, most often deviated from the straight lines. The slopes corresponding to the higher heating rates (2.5–20 K min^{-1}) were then also calculated. For the measurements carried out with equal cooling and heating rates, increasing slopes were observed for the lines corresponding to the various temperatures, in the order: T_e, T_p, T_m, T_f' and T_o. After a very slow cooling (1.25 K min^{-1}), the temperatures measured with various heating rates (q_h experiment) showed activation energies similar to the previous ones for T_e, T_p, T_m and T_o. In contrast, T_f' appeared to be independent of the heating rate, or de-

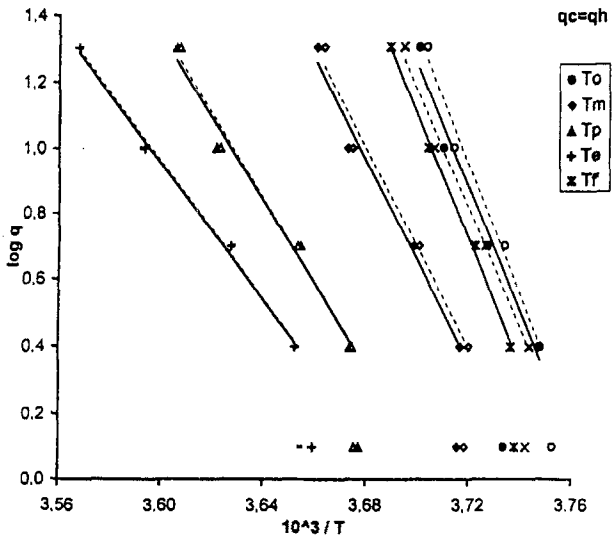

Fig. 3 "Arrhenius plots" of the temperatures T_o, T_m, T_p, T_e and T_f' for sorbitol samples subjected to cooling/heating rates ($q_c=q_h$). The regression lines illustrated are for cooling/heating rates between 20 and 2.5 K min^{-1}. Filled and empty symbols correspond, respectively, to two different samples

creased very slightly with it. In the experiments with varying cooling rates (q_c experiment), the temperatures T_e, T_p, T_m and T_o measured with a constant heating rate (10 K min^{-1}), were constant. T_f' values increased with cooling rate, with a high apparent activation energy. These changes were similar for fructose and sorbitol, although the respective Δh values could be different.

Discussion

The dependence of T_g on heating or cooling rate, according to equation [5], was demonstrated by Moynihan *et al.* [18] considering isobaric heating or cooling at a constant rate as the limit of a series of instantaneous, small temperature changes, each of which was followed by an isothermal hold, during which the structural relaxation process occurred. "Thermorheological simplicity" was assumed, i.e. temperature independence of the distribution of relaxation times. Equation [5] was derived with T_g defined as any particular value of the relaxational heat capacity, measured from heat-capacity cooling curves, in which cooling was started well above the transition region, or measured from heat-capacity heating curves obtained by reheating the glass from a temperature well below the transition region, after it had previously been cooled at a rate equal to the heating rate. Equation [5] could also be applied to T_f' measured on heating curves, following cooling processes at different rates [23].

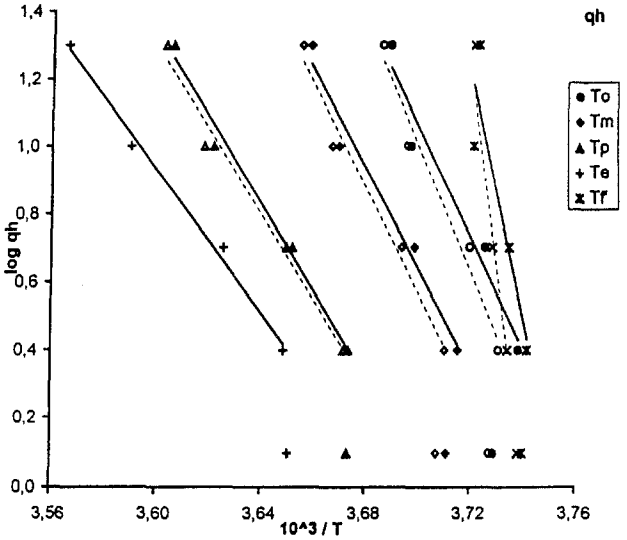

Fig. 4 "Arrhenius plots" of the temperatures T_o, T_m, T_p, T_e and T_f' for sorbitol samples subjected to reheating at various heating rates (q_h) after cooling at 1.25 K min^{-1}

The temperature values measured for $q_h = 1.25$ K min^{-1} were most often observed to deviate from the expected straight lines (Figs 3 and 4). Although the loss of instrument sensitivity at this low heating rate may have been responsible for some inaccuracy in the measurements, this would not explain the observed deviation, since the measured temperatures appear systematically "too high". It

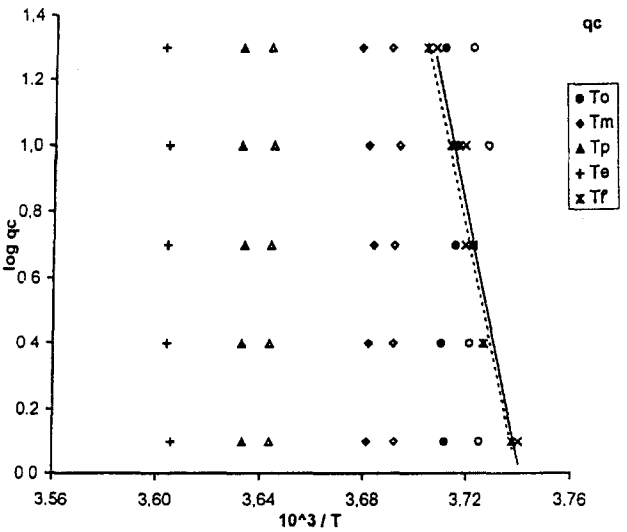

Fig. 5 "Arrhenius plots" of the temperatures T_o, T_m, T_p, T_e and T_f' for sorbitol samples subjected to reheating at 10 K min^{-1} after cooling at various rates (q_c)

must be stressed that temperature calibration was carried out several times during the investigation. An annealing effect during the heating process would also be excluded, since in this case, T_f' would be lower for the lowest heating rate; moreover the enthalpy recovery peak would also be higher. Part of the explanation (in addition to the inaccuracy) could be the non-Arrhenius behavior of the relaxation process, according to which the apparent activation energy increases with decreasing temperature. Table 1 shows the mean apparent Δh values for both the entire investigated cooling/heating rate range and the 2.5–20 K min^{-1} range, the latter being more similar to that used for conventional T_g determination (q=10 K min^{-1}).

The Δh values determined in the $q_c = q_h$ experiment were found to decrease in the order: T_o, T_f', T_m, T_p and T_e. Angell *et al.* [25] had also observed for sorbitol a value of Δh lower for T_p than for T_o (respectively, 330 and 389 kJ mol^{-1} for a cooling/heating rate range of 0.6–20 K min^{-1}). This is also to be expected from the non-Arrhenius behavior of the relaxation process.

The corresponding values of the fragility parameter (m) for sorbitol vary from 83 (for T_o) to 43 (for T_e), when the whole q range is considered, or from ca. 73 to ca. 38 for the restricted q range. The m values calculated from the Angell *et al.* [25] DSC data are ca. 64 for T_p. These values can be compared to data obtained from other types of measurements. The m value calculated for sorbitol from the B and T_o parameters of the VFT equation (viscosity measurements [22]) is ca. 94. Bohmer *et al.* [24] reported a value of m=93 calculated from dielectric relaxation data. The discrepancy with the DSC results may be explained either by the fact that enthalpy relaxation and mechanical or dielectric relaxations have different temperature coefficients and/or by the fact that the latter determinations imply an important temperature extrapolation.

Mechanical spectroscopy allows measurement in the T_g range. The apparent activation energy for the α relaxation is calculated from

$$\ln\frac{f}{f_o} = -\frac{\Delta h}{RT_\alpha}$$

where f is the frequency at which a maximum of the loss modulus (E'' or G'') is observed at the temperature of measurement. Figure 6 shows the variation of T_α (maximum of the loss modulus, G'') as a function of the measurement frequency, for sorbitol. A slight curvature can be observed, corresponding to the non-Arrhenius behavior of the α relaxation process.

The mean apparent activation energy for the tested frequency range is 253 kJ mol^{-1}, resulting in an m value of 49 (for a temperature range of 271–285 K). If we consider only the two lowest frequencies/temperatures, closer to the DSC temperature range, m ~59, a value consistent with the DSC results. Using Eq. [4] to calculate the WLF coefficient C_{2g}, from the m values obtained

Table 1 Apparent activation energies (Δh) determined for sorbitol and fructose from Arrhenius plots of the glass transition temperatures (T_o = onset, T_m=mid-point, T_p =peak, T_e =end-point) and of the limit fictive temperature (T_f') *vs.* cooling (q_c) and heating (q_h) rates (q_c and q_h in K min^{-1}). R^2 =regression coefficient for Δh, m=fragility parameter. The temperature values (K) for $q_c = q_h = 10$ K min^{-1} are indicated on the top line

	T_o	269		T_m	272		T_p	276		T_e	278		T_f'	270	
Sorbitol	Δh			Δh			Δh			Δh			Δh		
	kJ mol^{-1}	R^2	m	kJ mol^{-1}	R^2	m	kJ mol^{-1}	R^2	m	kJ mol^{-1}	R^2	m	kJ mol^{-1}	R^2	m
$q_c=q_h$															
20–1.25	425	0.97	83	342	0.92	66	288	0.94	55	235	0.94	44	405	0.93	78
	425	0.76	83	346	0.92	66	279	0.94	53	228	0.96	43	421	0.95	81
20–2.5	376	0.99	73	288	0.98	55	245	0.99	46	200	1.00	38	342	0.99	66
	355	0.98	69	292	0.98	56	239	0.98	45				360	1.00	70
q_h															
20–1.25	428	0.87		353	0.90		281	0.94		238	0.94	45			
	380	0.79		339	0.89		289	0.93							
20–2.5	354	0.97		295	0.98		239	0.98		202	0.99	38			
	313	0.96		282	0.97		245	0.99							
q_c															
20–1.25													728	0.92	141
													704	0.98	136

Table 1 Continued

Fructose	T_o	286		T_m	289		T_p	294		T_e	296		T_f'	287	
	Δh			Δh			Δh			Δh			Δh		
	kJ mol^{-1}	R^2	m	kJ mol^{-1}	R^2	m	kJ mol^{-1}	R^2	m	kJ mol^{-1}	R^2	m	kJ mol^{-1}	R^2	m
$q_c = q_h$															
20–1.25	436	0.78	80	354	0.94	64	301	0.94	54	273	0.93	48	390	0.97	71
	400	0.86	73	362	0.93	65	310	0.89	55	284	0.89	50	351	0.98	64
20–2.5	363	0.96	66	301	1.00	54	256	1.00	45	248	0.98	44	355	0.97	65
	330	0.98	60	305	1.00	55	257	0.99	46	236	0.97	42	343	0.96	62
q_h															
20–1.25	367	0.43		425	0.88		354	0.92		304	0.82	54			
	433	0.79		380	0.87		325	0.92		300	0.84	53			
20–2.5	380	0.92		352	0.97		297	0.99		252	0.98	44			
	348	0.99		327	1.00		274	1.00		248	0.99	44			
q_c															
20–1.25													803	0.87	146
													601	0.98	109

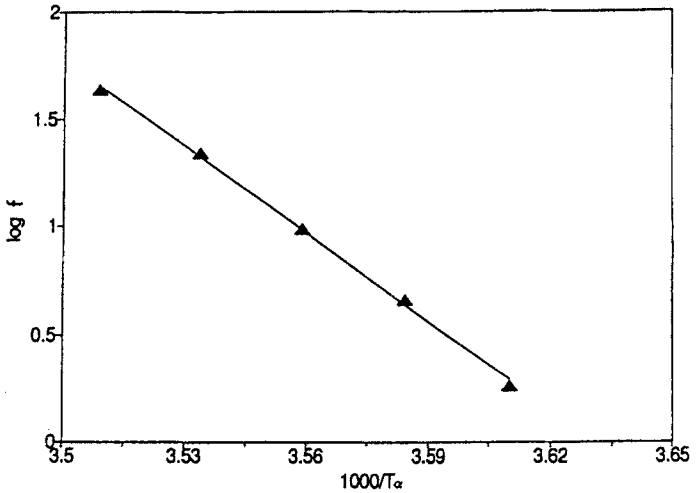

Fig. 6 "Arrhenius plot" of the temperature of the α relaxation (maximum of the loss modulus, G'') *vs.* the frequency of measurement for sorbitol

from the variation of T_f' (m=68), and assuming C_{1g}=16, one obtains C_{2g}=64, a figure slightly higher than the average value (or "universal" value, C_{2g}=51.4) calculated for a series of polymers [26].

It is worthwhile to note that the same comparison has been made for maltitol, between the apparent activation energy obtained from mechanical spectroscopy (α relaxation), i.e. 400 kJ mol^{-1}, and that deduced from DSC measurements, about 360 kJ mol^{-1}. The latter value was determined using the rate-cooling-dependence of T_g, which was defined as the temperature below which metastable equilibrium was no longer ensured [27].

The fragility parameter for fructose appears to be very slightly lower than that for sorbitol. The difference, however, appears to be due to the higher values of the transition temperatures in the case of fructose, the activation energies being similar or even higher for fructose than for sorbitol. Angell *et al.*[14] noted that fructose was stronger than glucose, on the basis of viscosity data from Ollett and Parker [28]. From the VFT parameters reported by the latter authors (viscosity measurements in the range 10^2–10^7 Pa.s), values of the fragility parameter would be 105 for glucose and 80 for fructose. It could have been expected that sorbitol would be more "fragile" than fructose, since the heat-capacity increment at the glass transition is much larger for sorbitol than for fructose: ca. 1 J g^{-1} K^{-1} for sorbitol and 0.7 J g^{-1} K^{-1} for fructose. Orford *et al.* [29] reported values of 251 and 151 kJ mol^{-1} K^{-1}, respectively, for these two materials. According to Angell [30], strong liquids exhibit small or sometimes undetectable changes in heat capacity at T_g, while the opposite is true for fragile liquids.

Angell [31], however, underlined the exceptional situation for alcohols, such as sorbitol, for which an intermediate fragility is associated with a high ΔC_p; alcohols should be classified as "thermodynamically fragile but kinetically strong" [31]. Most recently, the complex relaxation behavior of supercooled fructose was analysed and assigned mainly to tautomerization equilibria [32]. It might have been expected that these processes would induce some difference in the respective fragility values for fructose and sorbitol. Such a difference could not be detected in the present work.

In our experiments with a constant, slow cooling rate followed by rate-heatings (q_h experiment), the shape of the heating curves was significantly influenced by the heating rate, since the overshoot peak occurring at the end of the transition increased with the rate of rewarming. The enthalpy graph in Fig. 7 explains the origin of this overshoot peak. Very slow cooling enables the sample to reach a level of low enthalpy in the glassy state. If the sample is rewarmed at a rate significantly higher than the cooling rate, the experimental time is too short for the important structure/enthalpy recovery that has to be achieved; therefore, the hysteresis loop between the enthalpy curves for cooling

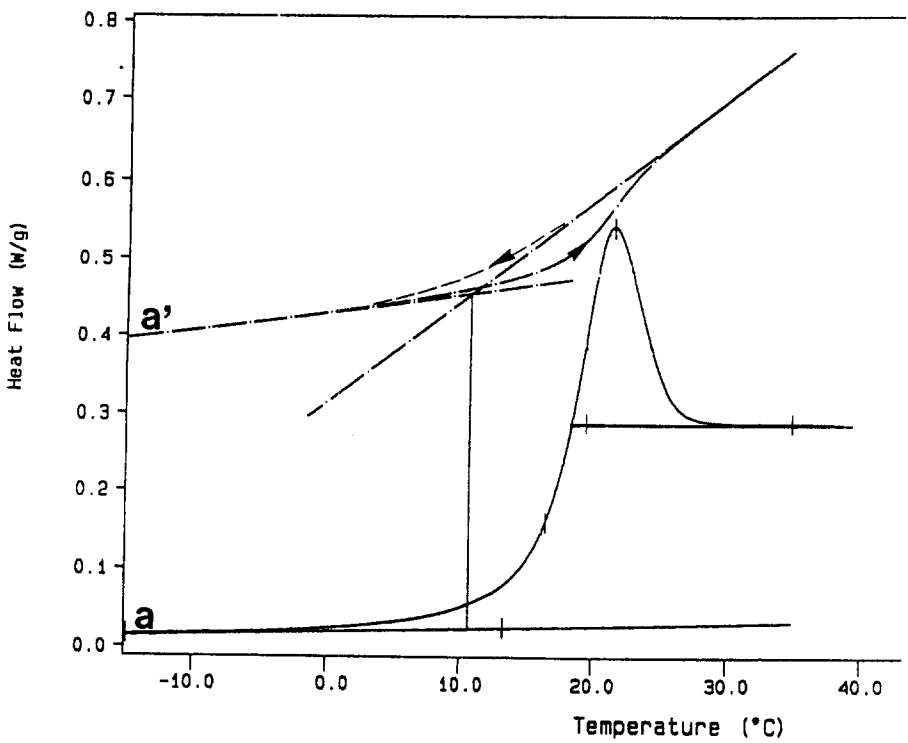

Fig. 7 DSC heating curve (a) for a fructose sample reheated at 20 K min^{-1} after cooling at 1.25 K min^{-1}. Curve a', showing the change in enthalpy during rewarming, was obtained by integration of the DSC curve. The indicated change during cooling is hypothetical

and heating is large. The enthalpy recovery occurs once the temperature has been sufficiently raised, giving rise to the endothermic peak. The increase of this enthalpy-recovery peak, when the ratio q_h/q_c is increased, has been observed for various materials and theoretically simulated [e.g. 33, 34]. Despite the change in shape of the curves, the slopes of the Arrhenius lines for T_o, T_m, T_p and T_e were not found to be significantly different from the corresponding slopes when $q_h/q_c=1$. These temperatures therefore appeared to be controlled mostly by the heating rate. The T_f', on the contrary, was found to be almost independent of the heating rate, which is consistent with the idea that this temperature is representative of the structural state of the glass.

These observations were confirmed in the q_c experiment, in which rate-coolings were followed by heating at a constant rate, $q_h=10$ K min^{-1}. The temperatures T_o, T_m, T_p and T_e showed constant values, whatever the cooling rate. In contrast, T_f' decreased with q_c. It is noticeable, however, that the corresponding activation energy values were significantly higher in these rate-cooling experiments, for both sorbitol and fructose, than they were in the experiments with $q_h/q_c=1$. The m values deduced from these high activation energies are greater than 100. With such values, sorbitol and fructose would exhibit very fragile behavior.

The difference in activation energies observed for T_f' in the "$q_c=q_h$" and "q_c" experiments corresponds to the fact that, after the same cooling rate, a different value of T_f' was observed depending on the heating rate: e.g. T_f' was higher in the cooling/heating cycle $q_c/q_h=2.5/10$ than in the cycle $q_c/q_h=2.5/2.5$; and higher with $q_c/q_h=20/20$ than with $q_c/q_h=20/10$. These differences could be due to some annealing effects (structural relaxation) occurring during the rewarming step, when the heating rate is lower than the cooling rate. After a relatively rapid cooling, some structure equivalent to an excess of enthalpy is "frozen in". If the subsequent rewarming is slower than the cooling step, this stage may be equivalent to some storage time at low temperature, during which some of the excess enthalpy is released (structural/enthalpy retardation, commonly referred to as "physical aging" [9]). As a result of this structural relaxation, a lower T_f' than expected is observed, as shown on Fig. 8. A similar difference, between the activation energies deduced from the variation of T_f' as a function of cooling rate and from a measurement of viscosity at temperatures approaching T_g, had been reported previously for ZBLA glass, a heavy metal fluoride glass; the value obtained from the DSC measurement (cooling rate between 0.5 and 80 K min^{-1}) was 1400 kJ mol^{-1} [33], and the one calculated from the viscosity variation (108–1012 Pa.s) was 875 kJ mol^{-1} [35].

These aging effects occurring during the course of rewarming point out the difficulty in using DSC rate-heating experiments to determine a fragility parameter as defined by Angell [1]. Measurements of T_g during cooling, which should be the most satisfactory approach to avoid this problem, did not provide consistent results in the present investigation. As an alternative approach, the

"q_h" experiment was designed so as to obtain a glassy material in a defined, constant structural state, and to determine the apparent activation energy in rate-heating experiments, particularly considering the temperature T_o, which

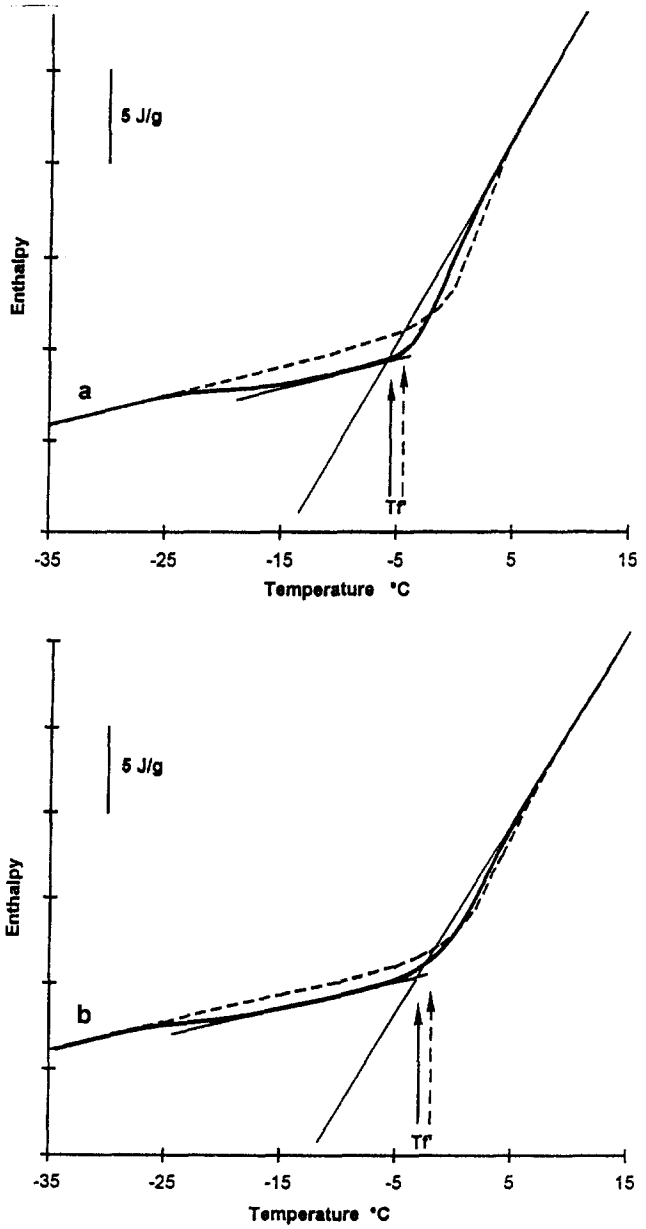

Fig. 8 Change in enthalpy during reheating for sorbitol: a) after cooling at 2.5 K min^{-1}, reheating at 2.5 K min^{-1} (solid line) or 10 K min^{-1} (dashed line); b) after cooling at 20 K min^{-1}, reheating at 10 K min^{-1} (solid line) or 20 K min^{-1} (dashed line)

we consider [12] to best represent the kinetic behavior of the glassy state. The data obtained for the apparent activation energy did not differ significantly from the results obtained in the "$q_c=q_h$" experiment. This was probably due to the fact that the cooling rate of 1.25 K min^{-1} resulted in only a limited aging.

Conclusion

The various temperature values used to characterize the glass transition depend significantly on the entire thermal history of the sample: cooling rate, storage at low temperature, heating rate. These variations in the absolute values, being a few degrees for the usual range of operating conditions, may be of no practical significance when considering the influence of temperature on kinetics in food materials.

The thermal history, however, results in important variations in the fragility parameter derived from DSC measurements. The limit fictive temperature appears to be an interesting parameter to characterize the liquid-to-glass transition temperature, and to determine the fragility parameter, necessary to model the kinetics in the temperature range above T_g. The apparent activation energy values, obtained in DSC experiments using equal rates of cooling and heating for the different temperature values used to characterize the glass transition (onset, mid-point, peak, end-point, limit fictive temperature), result in significantly different values for the fragility parameter defined by Angell [1, 14, 31]. Although these variations may be partly explained by the non-Arrhenius behavior of molecular mobility in the temperature domain above the glass transition, the influence of aging effects, occurring during heating scans performed at relatively low rates, should also be considered. More experiments should be carried out to provide a better understanding of the behavior observed for low cooling/heating rates. Current work under development, using a model to simulate heat-capacity curves, should be most useful to complement this understanding.

Efforts to obtain data through DSC cooling experiments should also be continued. It also seems desirable that DSC results should be compared to data obtained with other techniques, e.g. mechanical spectroscopy, which allows measurement during the cooling process, and also measurement of the activation energy for the α relaxation, independently of the cooling/heating rate. Although one must remember, when comparing results from the two techniques, that dynamic mechanical properties and enthalpy may have different relaxation behaviors (relaxation time and distribution of relaxation times) [36, 37], mechanical spectroscopy allows measurement of the activation energy for molecular mobility in the temperature range below T_g, as well as above. In fact, it has been proposed [38] that the temperature dependence of the dynamic behavior of glass-forming liquids undergoing structural changes should be better characterized by the parameter:

$$m^* = \frac{(\Delta h)^{T>T_g} - (\Delta h)^{T<T_g}}{RT_g}$$

Finally it must be emphasized that DSC has to be complemented by other techniques, if information on dynamic properties is desired. As was shown for mineral glasses [39], the T_g values determined by simple constructions on DSC curves do not necessarily correspond to the same relaxation time for different materials. Here again, a modelling approach would be useful to obtain more reliable relaxation times. Moreover, it is not possible, at the present time, to predict the temperature dependence of molecular diffusivity from knowledge of the material T_g, or even of its fragility parameter [40]; T_g and m values are useful landmarks, but they have to be complemented by diffusion measurements.

The limit fictive temperature could also be usefully employed to characterize the structural state of glassy food materials, and then to better understand the changes in texture, for instance, often observed in such products [41].

References

1 C. A. Angell, in Relaxations in Complex Systems, K. Ngai and G. B. Wright, eds., National Technical Information Service, US Department of Commerce, Springfield, VA 1985, p. 1.
2 H. Levine and L. Slade, Cryo-Letters, 9 (1988) 21.
3 H. Levine and L. Slade, in Water Science Reviews, vol. 3, F. Franks, ed., Cambridge University Press, Cambridge 1988, p. 79.
4 L. Slade and H. Levine, CRC Crit. Rev. Food Sci. Nutr., 30 (1991) 115.
5 L. Slade and H. Levine, in The Glassy State in Foods, J. M. V. Blanshard and P. J. Lillford, eds., Nottingham University Press, Loughborough 1993, p. 35.
6 Y. Roos and M. Karel, Food Technol., 45 (1991) 66.
7 J. L. Kokini, A. M. Cocero, H. Madeka and E. de Graaf, Trends Food Sci. Technol., 5 (1994) 281.
8 M. L. Williams, R. F. Landel and J. D. Ferry, J. Am. Chem. Soc., 77 (1955) 3701.
9 J. M. Hutchinson, Prog. Polym. Sci., 20 (1995) 703.
10 J. M. Hutchinson, Progr. Colloid Polym. Sci., 87 (1992) 69.
11 C. T. Moynihan, J. Am. Ceram. Soc., 75 (1993) 1081.
12 J. Perez, Physique et Mecanique des Polymeres Amorphes Lavoisier, Paris 1992.
13 C. A. Angell, L. Monnerie and L. M. Torell, Symp. Mat. Res. Soc., 215 (1991) 3.
14 C. A. Angell, R. D. Bressel, J. L. Green, H. Kanno, M. Oguni and E. J. Sare, in Water in Foods, P. Fito, A. Mulet and B. Mc Kenna, eds. Elsevier Appl. Sc., London 1994, p. 115.
15 ASTM Standard Method E 1356-91.
16 J. D. Menczel and T. M. Leslie, J. Thermal Anal., 40 (1993) 957.
17 I. M. Hodge, J. Non-Cryst. Solids, 169 (1994) 211
18 C. T. Moynihan, A. J. Easteal, J. Wilder and J. Tucker, J. Phys. Chem., 78 (1974) 2673.
19 H.Vogel, Physikal. Zeits., 22 (1921) 645.
20 G. S. Fulcher, Am. Ceram. Soc.,8 (1925) 339, 789.
21 G. Tammann and W. Hesse, Zeits. Anorgan. Allgem. Chem., 156 (1926) 245.
22 C. A. Angell and D. L. Smith, J. Phys. Chem., 86 (1982) 3845.
23 M. A. Debolt, A. J. Easteal, P. B. Macedo and C. T. Moynihan, J. Am. Ceram. Soc., 59 (1976) 16.
24 R. Böhmer, K. L. Ngai, C. A. Angell and D. J. Plazek, J. Chem. Phys., 5 (1993) 4201.
25 C. A. Angell, R. C. Stell and W. Sichina, J. Phys. Chem., 86 (1982) 1540.

26 J. J. Aklonis and W. J. MacKnight, Introduction to Polymer Viscoelasticity, Wiley-Interscience, New York 1983.
27 A. L. Faivre, (1996) submitted.
28 A. L. Ollett and R. Parker, J. Text. Stud., 21 (1990) 355.
29 P. D. Orford, R. Parker and S.G. Ring, Carbohydr. Res., 196 (1990) 11.
30 C. A. Angell, J. Phys. Chem. Sol., 49 (1988) 863.
31 C. A. Angell, J. Non-Cryst. Sol., 13 (1991) 131.
32 J. Fan and C. A. Angell, Thermochim. Acta, 266 (1995) 9.
33 C. T. Moynihan, A. J. Burce, D. L. Gavin, S. R. Loehr, S. M. Opalka and M.G. Drexhage, Polymer Eng. Sci., 24 (1984) 1117.
34 E. J. Donth, Relaxation and Thermodynamics in Polymers, Akademie Verlag, Berlin 1992.
35 W. C. Hasz and C. T. Moynihan, J. Non-Cryst. Solids, 40 (1992) 285.
36 J. Perez, J. Y. Cavaille, R. Diaz Calleja, J. L.Gomez Ribelles, M. Montlèon Pradas and A. Ribes Greus, Makromol. Chem., 192 (1991) 2141.
37 J. M. Hutchinson, J. Singh, R. W. Rychwalski, M. Delin, J. Kubat and C. Klason, 1st Int. Conf. Mechanics of Time Dependent Materials, Ljubljana (1995) 67.
38 J. Perez and J. Y. Cavaille. J. Non-Cryst. Sol., 172-174 (1994) 1028.
39 W. Pascheto, M. G. Parthun, A. Hallbrucker and G. P. Johari, J. Non-Cryst. Solids, 171 (1994) 182.
40 M. Le Meste, in Food Preservation by Moisture Control, G. V. Barbosa-Canovas and J. Welti-Chanes,eds., Technomic, Lancaster 1995, p. 209.
41 M. Le Meste, S. Davidou and G. Roudeau, J. Thermal Anal., 47 (1996) 1361.